Dynamic response of the cusp morphology to the interplanetary magnetic field changes: An example observed by Viking

M. Yamauchi and R. Lundin
Swedish Institute of Space Physics, Kiruna, Sweden

T. A. Potemra
Applied Physics Laboratory, Johns Hopkins University, Laurel, Maryland

Abstract. We present a unique Viking cusp observation during a period when the interplanetary magnetic field (IMF) observed by IMP 8 made a steplike change from southward to steady northward and subsequently back to steady southward again. The solar wind density and velocity were fairly steady during the entire period. Viking detected two independent plasma signatures. The first (equatorward part) is associated with southward IMF, and the second (poleward part) is associated with northward IMF. In the transition from the first signature to the second one, the ion data show an "overlapping injection" signature, i.e., two independent plasma populations exist on the same field lines and are well separated in the energy domain at any time and at any pitch angle. The second plasma population is found on the higher-energy side of the first population. A good relation between keV ion morphology and the field-aligned current pattern exists even though the particle cusp is undergoing a dynamic change. We discuss two possible scenarios for the present observation which involve the dynamic reaction of the cusp morphology to the stepwise change in the IMF condition.

(Received March 11, 1994; revised January 24, 1995; accepted January 24, 1995.)

(accepted manuscript)
J. Geophys. Res. 100(A5), 7661-7670, 1995 (copyright © 1995 by the American Geophysical Union)
https://doi.org/10.1029/95JA00333

1. Introduction

The overall large-scale particle morphology of the cusp is strongly controlled by solar wind conditions [e.g., *Woch and Lundin*, 1992a; *Newell and Meng*, 1994, and references therein]. The energy-latitude ion dispersion is one feature which is known to be governed by the interplanetary magnetic field (IMF) [e.g., *Reiff et al.*, 1977]. During periods of southward IMF, the characteristic energy of injected ions decreases toward higher latitudes while it remains constant ("stagnates") or even increases during periods of northward IMF. Such dispersion features become unclear for weak IMF conditions [*Yamauchi and Lundin*, 1994]. Other features that reflect the IMF conditions include the characteristics of the cleft acceleration region [*Woch and Lundin*, 1992a], electron signatures poleward of the cusp [*Hardy et al.*, 1986; *Yamauchi and Lundin*, 1993], and the nature of the mantle cusp. These features are found consistently regardless of the existence of many embedded temporal injections, and they may even be used to monitor the IMF conditions [*Yamauchi and Lundin*, 1994].

With the knowledge of the overall large-scale particle morphology, a single satellite observation may in principal detect dynamic responses of the cusp morphology to changes in IMF conditions if the change takes place during the satellite's cusp traversals. For studies of the temporal variation of the cusp morphology, a mid-altitude satellite such as DE 1, Viking, or Akebono has an advantage compared to a low-altitude satellite because the former stays within the cusp much longer (10 to 20 minutes) than the latter does (less than a few minutes). Yet even with mid-altitude satellites, it is still difficult to identify a dynamic response event, because such a study requires stepwise changes in the solar wind condition at the right time. We found only one such example in several hundreds of Viking cusp traversals (we examined all noon-midnight traversals in which one may see plasma signatures of both northward and southward IMF types at different latitudes). In this example, the IMF changed stepwise from southward to northward and back to southward, and we observed a change of the cusp morphology which corresponds to either the southward-to-northward change or the northward-to-southward change of the IMF direction.

2. Observations

Plate 1 shows the Viking ion and electron energy-time spectrograms for 70 - 500 eV electrons and 50 eV - 30 keV ions for orbit number 1032 (August 28, 1986). Details of the Viking particle instrument can be found in *Geophys. Res.*

Lett. Special Issue [1988]. Figure 1 shows the solar wind condition observed by IMP 8 during this period. The IMF B_Z jumped from -5 nT to +5 nT instantaneously at 1125 UT and back to steady southward (B_Z = -4 nT) at 1142 UT, whereas the solar wind velocity and density stayed fairly constant.

The Viking ion observations during 1143-1150 UT show that the cusp ion population is strongly influenced by a southward IMF. The satellite detected a sudden transition of ion population from tens of keV ring current ions to > 1 keV cusp injecting ions (in the acceleration region) at 1143 UT, and subsequently a decreasing ion dispersion signature (decreasing characteristic energy toward higher latitude) inside the cusp proper. Immediately equatorward of this transition (1143 UT), keV upward ion beams are seen. All these are cusp characteristics for southward IMF conditions [*Reiff et al.*, 1977; *Burch et al.*, 1982; *Woch and Lundin*, 1992a]. However, there is still an uncertainty as to whether this part (1143-1150 UT) reflects only a southward IMF or includes some northward IMF effect. For example, the ion energy of the inverted V-shaped pattern after 1147 UT does not drop in a consistent way which is contrary to what is observed in a typical ion dispersion pattern of southward IMF conditions [cf.,*Yamauchi and Lundin*, 1994, Figure 13], although this may be attributed to another mechanism such as field-aligned potential drops above or below the spacecraft (downward field above or upward field below). If such field-aligned potential drops exist, one may also expect ion heating to occur due to wave turbulence [e.g., *André et al.*, 1990] caused by precipitating particles through such structures. In fact, the upward ion conics (100 eV to 1 keV) are seen at 1146:40-1151:00 UT in the lower panel of Plate 1b. Such ion conics or elevated ion beams are always observed at the leading edge of new ion signatures in the cusp (e.g., Figure 1a of *Woch and Lundin* [1992a]). Therefore the rather high energy of the V pattern (at energies between 300 eV and 2 keV) after 1147 UT in Plate 1 can be attributed to the energization mechanism associated with the second injection, instead of a northward IMF condition. We need more information to establish whether the first ion signature (1143-1150 UT) contains some effects of northward IMF [*Yamauchi and Lundin*, 1993, 1994]. The plasma convection (electric field) direction is one important piece of information. However, the electric field instrument was switched off during this period, and the ion drift direction obtained from the particle data (not shown here) is not conclusive. Hence we may only conclude that the ion signature for 1143-1150 UT is strongly affected by southward IMF. Corresponding southward IMF at the IMP 8 location is observed before 1125 UT and after 1142 UT.

Starting with weak fluxes of downward keV ions at 1146:50 UT, the second ion signature (1147-1153 UT) shows quite a different morphology: there is no distinct mantle population [*Kremser and Lundin*, 1990]; the "cusp poleward

edge" is observed at 1154 UT [*Yamauchi and Lundin*, 1993]; the ion energy-time dispersion is "stagnant" [*Yamauchi and Lundin*, 1994]. These are characteristics for northward IMF conditions, and no effect of southward IMF can be found during the second ion signature. Hence this part corresponds to the steady northward IMF for 1125-1142 UT at the location of IMP 8.

The first (1143-1150 UT) and the second (1147-1153 UT) ion signatures overlap each other composing a typical "overlapping injection" signature [*Yamauchi and Lundin*, 1994; *Norberg et al.*, 1994]. These two ion signatures are well separated in energy at any pitch angle as can easily be seen in the lower panel of Plate 1. They are clearly independent of each other but are yet located on the same field line over one degree of latitudinal range. The detail of the overlapping part can be seen in the lower panel. There are two types of double intensity peaks in the figure. The first one (1146-1147 UT) is caused by different masses of the injected particles. The energies-per-charge for these two peaks are at constant ratio (one to two) at any point, indicating that they are protons and alpha particles. We can even see another peak at the ratio of 4 (not discernible in Plate 1), indicating helium ions. The second double peak structure (1147-1149 UT) is clearly different from the first one. Apparently, what we call "overlapping injection" signature is not attributed to different ion species contrary to the suggestion by *Burch et al.* [1982]. From this and the other reasons mentioned above, the overlapping injection signature during 1147-1150 UT is caused by two independent plasma populations on the same field line with two different downward velocities (at a fixed space-time point). Thus magnetosheath plasma was injected on these field lines at two different times.

The second ion signature is found on the higher energy side at all pitch angles. *Yamauchi and Lundin* [1994] statistically showed that overlapping injections most likely indicate a time sequence of injections; i.e., the plasma with higher characteristic energy is injected later than those with lower energy. However, we may not conclusively say so for a single observation under an unusual IMF condition: the present overlapping signature could simply be due to spatial mixing. Let us examine both possibilities:

If what Viking detected was a temporal change, i.e., if Viking moved slowly enough to detect "injections," the second plasma population (1147-1153 UT) characterized by northward IMF must have originated after the first plasma population (1143-1150 UT) associated with southward IMF, and hence the energies of overlapping populations reflect the time sequence [*Yamauchi and Lundin*, 1994]. This leads to a scenario as shown in Figure 2. The first ion signature is associated with the first southward IMF period before 1125 UT at IMP 8. In this figure, we assumed that the cusp position moved poleward continuously without a "jump" when the northward IMF reached the high-

altitude cusp, and hence the leading edge of the new injection stems from the equatorward boundary of the "old" cusp. One might claim another possibility that the cusp position "leaps" instead of moving continuously, but we are at present unable to integrate this "leap" picture into the existing cusp models (see discussion)

The interpretation illustrated in Figure 2 explains the particle data well except for the timing. The constant solar wind velocity indicates that the stepwise IMF change is caused by the crossing of the heliospheric current sheet which is flipping up and down near the ecliptic plane. The "fold" of the current sheet then probably lies in the direction from $+X$ and $-Y$ to $-X$ and $+Y$. If this is the case, the northward IMF should have arrived at the Earth and at IMP 8 nearly simultaneously at around 1125 UT, implying that the cusp has been strongly influenced by southward IMF during the subsequent 25-30 min. Since a 1 keV proton (≈ 440 km/s) travels 10 R_E (field-aligned length of the cusp) within a few minutes, this is unrealistic.

This timing problem can be resolved if the "fold" of the current sheet lies in a different direction, e.g., from $+X$ and $+Y$ to $-X$ and $-Y$. In fact, the IMF B_Z component is much larger than the IMF B_Y component, which indicates that this particular heliospheric boundary crossing was somewhat unusual. The special "folding" direction is possible if, for example, a localized magnetic disturbance near the sun propagates along Parker's spiral as an Alfvén wave. In this case, the arrival time of northward IMF turning at IMP 8 location (Y = -30 R_E) was much earlier than that directly upstream of the Earth (Y = 0 R_E). Therefore we may expect a 10 to 15 minute delay in arrival of the northward IMF at the exterior cusp, and may expect a northward IMF turning there at around 1135-1140 UT.

The "overlapping injection" signature may not necessarily be due to temporal effects, but could be related to spatial effects. The observed energy may simply indicate the source energy of each ion population instead of the sequence of injection time at the source region, although we cannot at present specify the mixing mechanism. In this interpretation, Viking must have moved fast enough to take a "snapshot" of the cusp as shown in Figure 3a. The equatorward ion signature (1143-1150 UT) may correspond to either the first southward IMF period before 1125 UT at IMP 8 (Figure 3b) or the second southward IMF period after 1142 UT at IMP 8 (Figure 3c). The latter case does not have the timing problem concerning the arrival of the southward IMF which is observed at 1143 UT by Viking. It could even be earlier than 1143 UT depending on the direction of the "fold" of the heliospheric current sheet. In this case, two different plasmas with different source regions mix as the result of a poleward propagation of a new "southward IMF" type population. In Figure 3, we have again assumed a continuous motion of the cusp boundary

without a "jump." Such a continuous motion during southward IMF conditions is reported by *Nilsson et al.* [1994].

The second scenario illustrated in Figure 3c has, however, the other type of timing problem. The "northward IMF" type cusp plasmas contain a field-aligned downward component until 1153 UT, and the ions detected at 1153 UT must have originated at the high-latitude magnetospheric boundary region before southward IMF swept there, whereas the southward IMF has already arrived at the Viking position before 1143 UT. Since a 1 keV proton travels 40 R_E in 10 min, the protons detected at 1153 UT must have originated somewhere significantly tailward. We may not argue at the present time whether this is possible or not.

The field-aligned currents (FACs) provide another clue. The magnetic field is shown in Plate 1 as thin solid lines. The rather flat north-south component guarantees that the slope of the east-west component is a good estimate of the current density. Since the particle cusp (seen by keV ions) is in a state of rapid morphological change, it might be unwise to adopt the quasi-steady concept of large-scale FACs. The FACs are normally carried by low-energy (eV) electrons for large-scale FACs and by field-aligned keV electron beams for localized intense FACs [e.g., *Potemra et al.*, 1987]. It is not straightforward to relate the keV ion morphology and the FAC pattern. However, the overall FAC pattern is in good agreement with the traditional large-scale FAC pattern which has a good relationship to keV ion patterns.

A broad and rather weak downward current before 1143 UT coexists with 10 keV magnetospheric ions (Plate 1) and electrons (not shown here) of the ring current origin. The oppositely directed (upward) intense and confined current at 1143-1145 UT coexists with energized magnetosheath plasma of the boundary cusp [*Woch and Lundin*, 1992a]. The 100 nT perturbation observed here is a typical value in Viking observations of large-scale FACs in the cusp-cleft region [e.g., *Erlandson et al.*, 1988]. Confinement and intensification of the dayside region 1 FAC are characteristics of southward IMF [*Iijima and Potemra*, 1976; *Woch et al.*, 1993]. Poleward of this, there is another weak and broad downward current until 1156 UT. This is not clear in Plate 1 but is clear in Plate 1 of *Ohtani et al.* [1995] (see the figure caption). *Ohtani et al.* [1995] in a study of simultaneous particle and magnetic field data acquired by Viking and DMSP-F7 satellites have included the same Viking orbit 1032 studied here. At 1156 UT, we see a small but clear change of slope in B_E, indicating that there exists an FAC before 1156 UT but none after 1156 UT. The equatorward end of this FAC (1145 UT) matches the start of the upward moving ions with inverted-V shape. Consequently, Viking crossed three FAC sheets which flow downward, upward (intense), and downward (less intense but broad) from equatorward to poleward, and the observed features are quite

consistent with those of the postnoon region 2, (cusp part) region 1, and (cusp part) region 0 FACs [e.g., *Yamauchi et al.*, 1993a] during southward IMF. Furthermore, the good correspondence between different FAC regions (especially, the region 1 and the region 2 FACs) and different plasma regions indicates that the main part of the observed FACs are traditional quasi-steady state large-scale FACs. We delineate the corresponding ΔB by a heavy solid line in Plate 1.

Viking is located sufficiently close to local noon so that the flow directions of the large-scale FACs are expected to reflect the IMF B_Y component. The observed flow directions agree with those of the large-scale FACs in the midnoon sector during a dawnward IMF [*Iijima and Potemra*, 1976]. This correspondence is valid for both northward and southward IMF conditions. In the present case, the dawnward IMF occurs together with a southward IMF (before 1125 UT and after 1142 UT at IMP 8). Thus the flow directions support the above interpretation that the observed FAC system reflects a southward IMF condition.

We now compare the FAC observation to the scenarios discussed in Figures 2 and 3. If the equatorward particle signature corresponds to the first southward IMF period before 1125 UT (cf. Figure 2 or Figure 3b), we would expect existence of a traditional large-scale FAC system for a southward and dawnward IMF condition because the IMF was fairly steady for more than half an hour before the Viking traversal. The observed FAC system agrees with this prediction. On the other hand, the alternative interpretation (Figure 3c) poses the following difficulty. The FAC system must have developed as quickly as keV particles have injected into the cusp. Although an independent bulk plasma signature normally accompanies some FACs [*Woch and Lundin*, 1992b; *Potemra et al.*, 1992], they are normally mesoscale FACs and only rarely large-scale ones (we denote a FAC "mesoscale" if it is smaller than the traditional large-scale FACs). The total current intensity of these "injection-related" FACs is much smaller than that of the typical large-scale FAC (see Figure 15 of *Lundin et al.* [1991]). Thus the well-developed FAC system ($\Delta B \approx$ 100 nT in cusp) is difficult to be interpreted by the second scenario (Figure 3c). Consequently, the evidence appears to support the first scenario better (Figure 2 or 3b).

If the poleward plasma population is due to a new injection (cf. Figure 2), it is expected to accompany some FACs which are less intense than the large-scale FACs as mentioned above. Since the IMF B_Y component was positive during the period of northward IMF (1125-1143 UT at IMP 8), we expect an eastward ΔB inside the poleward (northward IMF type) plasma region [*Yamauchi*, 1985]. A possible candidate for such an eastward ΔB deviation (i.e., a pair of FACs) is delineated by a dotted line in Plate 1. If so, this

mesoscale FAC system can also be an initial signature of a new large-scale FAC system for northward IMF. Its equivalent ionospheric convection pattern is well known to develop rather quickly in response to changes in the IMF condition [*Clauer and Banks*, 1986; *Knipp et al.*, 1991].

Plate 1 (orbit 1032) is a unique observation of the cusp response to solar wind dynamics. No other Viking cusp traversal occurred right on time when the IMF exhibited a stepwise change. However, if we include periods when the IMF data were either missing or highly disturbed, we can find several Viking cusp traversals with transit events showing mixtures of different large-scale morphologies. We refer to them as "hybrid cusps" hereafter. Plate 2 (August 23, 1986) is an example of such a hybrid cusp. The IMF is unavailable, but *AE* is nearly 500 nT indicating a southward IMF condition some time during or before the Viking traversal.

Viking observed a typical low-latitude boundary layer and cusp ion signature which is associated with a southward IMF until 77.4 invariant latitude (Inv) during its poleward traversal over the dayside cusp-cleft region. The same plasma population is present up to 77.8 Inv (1802 UT) if one traces the mirror reflected component (inverted V-shaped pattern). Meanwhile, new downward flowing ions are found at around 1800-1801 UT, first a small downward flowing ion population at 77.3 Inv, followed by a more intense one at 77.5 Inv, as are indicated by the arrows. These downward ions are probably from the same plasma population. The new ion signature is accompanied by intense upward ion conics (300 eV to 1 keV at 1800:00 UT and 1800:40 UT) and a discontinuity in the eastward component of the magnetic field (1800:25 UT, marked by the vertical dashed line). After 1802 UT, the entire ion and electron signatures exhibit features often observed for northward IMF, e.g., a rather flat ion characteristic energy (this is for weakly northward IMF [*Yamauchi and Lundin*, 1994]), an acceleration region poleward of the cusp at 79.3 Inv [*Woch and Lundin*, 1992a], upward keV ionospheric ion beams instead of ordinary upflowing mantle ions (< 100 eV, wider in the pitch angle) up to 81.1 Inv, and intense polar showers from 81.2 Inv to beyond the right end of Plate 2 [*Hardy et al.*, 1986].

Thus this cusp traversal contains at least two different large-scale ion populations, one on the equatorward side corresponding to southward IMF, and the other on the poleward side corresponding to northward IMF. These two populations overlap between 77.3 Inv and 77.8 Inv. However, the details of the overlapping injection signature is different from Plate 1. The second plasma population is moving primarily downward (injection) whereas the first population is moving primarily upward (mirror reflected), and it is not clear if they exist simultaneously at the same pitch angle with different energies. In Plate 1, two ion populations are found at the same pitch angles in both

downward and upward directions.

The FAC system in Plate 2 is more complicated than that in Plate 1. The north-south magnetic field component fluctuates considerably, and the entire cusp is dominated by mesoscale FACs instead of the well-defined large-scale FACs. Certainly, the observed FACs are hardly interpreted in terms of the quasi-steady state region 0, 1, and 2 sheet FACs. The traditional three sheet FACs may exist but we cannot recognize them in the figure. Yet, the most prominent mesoscale FACs are found to coexist with the newly injecting plasma. A pair of downward and upward FACs appears where the strong particle influx associated with southward IMF exists (see dotted line in Plate 2), and another pair of FACs (dotted line in the figure) appears where the second particle injection associated with northward IMF exists. Thus a good correspondence between the keV ion morphology and the mesoscale FAC pattern is again obtained during the transit period. The poleward current system with northward IMF signature is more developed than the equatorward one with southward IMF signature. These two current systems are separated by a strong field-aligned current sheet at 1800:25 UT as mentioned above, indicating that two mesoscale FACs are independent of each other.

3. Summary and Discussion

We have two scenarios (cf. Figures 2 and 3) for the dynamics of the "hybrid cusp" of Plate 1. The first scenario is that the equatorward plasma signature corresponds to the first southward IMF period before 1125 UT at IMP 8 location (Figures 2 and 3b), and this explains the observations of both particles and magnetic fields. The overall FAC system can be a large-scale (quasi-steady state) one for a southward and dawnward IMF condition in this case. A special explanation is needed for the time gap (20 min) between the IMF change at IMP 8 location and its detection by Viking. This timing problem does not present in the second scenario in which the equatorward plasma signature corresponds to the second southward IMF period after 1142 UT at IMP 8 location (Figure 3c). However, this scenario requires many unusual conditions as follows. The southward IMF type cusp expands poleward with a speed less than that of the Viking satellite; the plasma with northward IMF remains far downstream (>40 R_E) of the exterior cusp and maintains the precipitation from there for more than 10 min after the first ion signature with southward IMF started; the large-scale FAC system (even the region 2 FAC) develops almost instantaneously with the keV ion injection; and the two different plasmas with different source regions just mix as a result of poleward propagation of a new ion population with southward IMF.

As mentioned earlier, we cannot rule out the possibility that the equatorward

ion signature reflects some northward IMF effect although the ion signature is significantly influenced by the southward IMF. If this is the case, the particle cusp must have responded to the northward turning of IMF in two steps. We do not go into detail on this interpretation because the supporting evidence is not strong. Furthermore, the basic dynamics for this case is very similar to those for the above two scenarios.

Even with some ambiguities, the following facts remain for the cusp observation in Plate 1: (1) The stepwise IMF change leads a new independent plasma population which is separated from the old population in the energy-time domain. (2) Over one degree of latitudinal width, the new population is found on the same field lines as the old population. Such an "overlapping injection" is not an artifact of different ion masses. (3) Each independent ion signature separates a mesoscale or large-scale FAC system during the transit period. Hence the FAC generation mechanism is related to the cusp particle formation mechanism.

We should note here that some hybrid cusp observations by Viking (e.g., Plate 2) show different characteristics during the transition stage. There are certainly different forms of the hybrid cusp. It is also possible that we missed certain types of hybrid cusps without overlapping structures. Therefore it is too early to conclude that the cusp in a transition stage should have overlapping injections.

Let us compare the present result with existing cusp models. We just consider here two models: merging-related cusp models [*Burch et al.*, 1982; *Reiff et al.*, 1977] and the wave-assisted cusp model [*Yamauchi and Lundin*, 1994]. Let us first consider the merging-related cusp models. Since the overlapping structure is generally not consistent with the "frozen-in" concept [*Norberg et al.*, 1994, *Yamauchi and Lundin*, 1994], we need a special explanation for this structure. One obvious way to explain the observation is to combine a bursty injection mechanism [*Lemaire*, 1977] to the existing quasi-steady state cusp models. Another possible scenario could be **"re-reconnection"** on the same geomagnetic field lines at different places and different times: the first particle injection from the magnetosheath region with southward IMF takes place somewhere at the dayside, whereas the second one for northward IMF takes place somewhere at the poleward side of the cusp. However, one problem remains with the "re-reconnection" scenario. In Figure 2, the "overlapping injections" occurs because the source region of the cusp particles moves poleward faster than the "velocity" of the old flux tube (i.e., poleward convection velocity). The old flux tube is, however, expected to convect poleward with the magnetosheath velocity (because these open field lines are "frozen-in" to those in the southward IMF region in the magnetosheath) so that the northward IMF region never overtakes this flux

tube (the solar wind velocity was constant). The authors have not yet found a way to get around this problem. This is why we did not employ a "leap" picture in Figure 2.

Next we consider the wave-assisted cusp model: the cusp boundary moves dynamically back and forth [*Potemra et al.*, 1992] depending on the solar wind conditions or even spontaneously, as if the cusp boundary is assisted by a standing wave or shock (Figure 14 of *Yamauchi and Lundin* [1994]). Since this is rather a new model, we give a brief explanation here. A detailed explanation will be found in the work by *M.Yamauchi and R. Lundin* [A model of plasma flow in the exterior cusp, submitted to *Journal of Geophysical Research*, 1993 **=> https://doi.org/10.1016/S0079-1946(97)00203-6**].

The wave-assisted cusp model may explain many cusp observations as well as other cusp models do. According to numerical simulations [*Yamauchi*, 1994] and analytical studies [*Yamauchi et al.*, 1993b], if a standing compressional wave or shock (in our cases, it is magnetosonic mode) exists at the equatorward boundary of high-altitude cusp, it can generate simultaneously the region 1 and region 0 FACs which coexist with cusp particles [*McDiarmid et al.*, 1979]. The numerical simulation also shows active "wings" with a wake structure which is inherent to large-amplitude waves, and shows a rather quiet "nose" (or "head") where the FACs are minimized. The "wings" should correspond to the active and transient cusp auroras in the boundary cusp or LLBL [*Sandholt et al.*, 1986; *Yamauchi and Lundin*, 1994], whereas the "nose" corresponds to the midday gap of aurora [*Dandekar and Pike*, 1978] in the rather stable cusp proper [*Yamauchi and Lundin*, 1994]. The wave-assisted cusp model also predicts the dramatic effect of the solar wind dynamic pressure on the cusp morphology [*Newell and Meng*, 1993] through the wave amplitude, strong seasonal effects because of geometry [*Newell and Meng*, 1988; *Yamauchi and Araki*, 1989], and the standing Alfvén waves at the equatormost part of the cusp [*Maynard et al.*, 1991]. Thus the model is consistent with the low-altitude cusp observations. High-altitude in situ observations have not been sufficient to examine the existence of such a structure; yet a shock-like structure other than the magnetopause is sometimes found at the cusp boundary [*Lundin*, 1985].

The obvious question is then whether it is theoretically feasible to have such a "standing wave or shock" there. First, we should note that the magnetosheath flow is expected to become supersonic near the cusp. This is predicted by all gasdynamic (GD) models, and the prediction is valid for magnetohydrodynamics too. Furthermore, GD predicts a secondary shock in front of the high-altitude cusp [*Walters*, 1966] because of the special geometry of the magnetopause there. Extending this idea and considering more realistic boundary conditions, one may construct a more realistic flow passage from the

magnetosheath through the high-altitude cusp (entry layer or exterior cusp) to the plasma mantle or LLBL. Let us take a "stream tube" of such a flow [e.g., *Courant and Friedrichs*, 1948]. The cross section of the stream tube would be smallest near the high-altitude cusp, making the entire flow geometry resemble a de-Laval nozzle. Then one can analyze the flow profile in a similar way to the flow inside a de-Laval nozzle, i.e., using the mass-, momentum-, and energy-conservation laws [e.g., *Courant and Friedrichs*, 1948]. The difference is that we consider a magnetized plasma instead of a neutral fluid. This difference does not affect the solution unless the magnetic stress force drastically modifies the conservation laws. This is not very likely to be the case because the strength of the geomagnetic field minimizes significantly near the high-altitude cusp in any geomagnetic field models [e.g., *Stasiewicz*, 1991]. Then, one may use conservation laws as the zero'th approximation, and find a shocked-flow solution and a smooth-compression (i.e., a large-amplitude wave) solution as the major solutions (Figure 15 of *Yamauchi and Lundin* [1994]).

Now, we incorporate the wave-assisted cusp model into the present observation. Since the boundary of high-altitude cusp is not a solid surface but a standing compressible structure, it allows a direct plasma entry. The magnetic sector boundary may also transmit, simultaneously stimulating a poleward displacement of the cusp boundary. Note that the velocity of this displacement is slower than the plasma flow velocity. One may then have a scenario for the present observation (Plate 1) as shown in Figure 4. The low-altitude part of the figure is the same as Figures 2 and 3b. In the lower part of Figure 4, we have both an "old" boundary (thin line) and a "new" boundary (think line) because high-energy particles affected by northward IMF overtake low-energy particles affected by southward IMF. The "new" boundary in the figure approximately represents a single field line. The low-altitude cusp boundary moves poleward after the new boundary reaches the ionosphere. Apparently a "slip" is presumed between the incoming magnetosheath plasma flow and the magnetospheric field lines, like a Hartmann's flow. One may describe this as "gradual re-reconnection", but the mechanism is quite different from the "re-reconnection" mentioned above. The idea of "slip" is observationally supported by *Woch and Lundin* [1992a], who showed that the poleward convection velocity inside the low-altitude cusp is not very large even for southward IMF. They found that the dawn-dusk deflection is more significant than poleward flow. This means that the velocity of the flux tube inside the low-altitude cusp is slower than the velocity of the same flux tube in the exterior cusp. From the low-altitude point of view, the source region (sector boundary) moves faster than the cusp boundary. The "slip" of convection thus allows the source region to move faster than the ionospheric

convection. The overlapping injections may occur as a natural consequence.

4. Conclusions

We have presented an example of "hybrid cusps" (Plate 1), transitional stages of the cusp, when the IMF changes stepwise from southward to northward and back (Figure 1). Viking observed two different types of plasma signatures: one strongly related to southward IMF, and the other strongly related to northward IMF. These two plasmas overlap on the same field lines for three minutes, but they are still well separated from each other in the energy domain. While the second ion signature (1147-1153 UT) is obviously related to the period of steady northward IMF (1125-1142 UT at IMP 8), we are not able to conclude whether the first ion signature corresponds to the first southward IMF period (before 1125 UT at IMP 8) or the second southward IMF period (after 1142 UT). We then have proposed two scenarios: 1. The second ion population swept over the first one as shown in Figure 2 and Figure 4, and the equatorward cusp boundary oscillated back and forth responding to the change in the solar wind conditions. 2. The equatorward ion population associated with southward IMF expanded poleward with a speed lower than that of the Viking satellite as shown in Figure 3c, and two different plasma populations simply mixed at the boundary.

The "hybrid cusps" do not always have the same characteristics: the overlapping morphology in Plate 1 is different from that in Plate 2 although the latter is not supported by IMF data. Each independent plasma signature (associated to northward and southward IMFs) in the transit stage seems to accompany mesoscale (rather temporal) or large-scale (quasi-steady state) FACs.

Acknowledgments. The Viking project is supported by the Swedish National Space Board. The Viking magnetic field instrument was supported by the Office of Naval Research. The IMP-8 data were provided by R. P. Lepping and A. J. J. Lazarus through WDC-A. The AE index is provided by WDC-C2 for geomagnetism at Kyoto University. The authors thank S. Ohtani, M. Hirahara, C. Nairn, and both referees for helpful comments.

The Editor thanks M. F. Smith and another referee for their assistance in evaluating this paper.

References

André, M., G. B. Crew, W. K. Peterson, A. M. Persoon, C. J. Pollock, and M. J. Engebretson, Ion heating by broadband low-frequency waves in the cusp/cleft, *J. Geophys. Res., 95*, 20809-20823, 1990.

Burch, J. L., P. H. Reiff, R. A. Heelis, J. D. Winningham, W. B. Hanson, C. Gurgiolo, J. D. Menietti, R. A. Hoffman, and J. N. Barfield, Plasma injection and transport in the mid-altitude polar cusp, *Geophys. Res. Lett., 9*, 921-924, 1982.

Clauer, C. R., and P. M. Banks, Relationship of the interplanetary electric field to the high-latitude ionospheric electric field and currents: Observations and model simulation, *J. Geophys. Res., 91*, 6959-6971, 1986.

Courant, R., and K. O. Friedrichs, *Supersonic Flow and Shock Waves*, 464 pp., Interscience, New York, 1948.

Dandekar, B. S., and C. P. Pike, The midday, discrete auroral gap, *J. Geophys. Res., 83*, 4227-4236, 1978.

Erlandson, R. E., L. J. Zanetti, T. A. Potemra, P. F. Bythrow, and R. Lundin, IMF B_y dependence of region 1 Birkeland currents near noon, *J. Geophys. Res., 93*, 9804-9814, 1988.

Hardy, D. A., M. S. Gussenhoven, K. Riehl, R. Burkhardt, N. Heinemann, and T. Schumaker, The characteristics of polar cap precipitation and their dependence on the interplanetary magnetic field and the solar wind, in *Solar Wind-Magnetosphere Coupling*, edited by Y. Kamide and J. A. Slavin, pp. 575-604, Terra Scientific, Tokyo, 1986.

Iijima, T., and T. A. Potemra, Field-aligned currents in the dayside cusp observed by Triad, *J. Geophys. Res., 81*, 5971-5979, 1976.

Knipp, D. J., A. D. Richmond, B. Emery, N. U. Crooker, O. de la Beaujardiere, D. Evans, and H. Kroehl, Ionospheric convection response to changing IMF direction, *Geophys. Res. Lett., 18*, 721-724, 1991.

Kremser, G., and R. Lundin, Average spatial distributions of energetic particles in the mid-altitude cusp/cleft region observed by Viking, *J. Geophys. Res.*, 95, 5753--5766, 1990.

Lemaire, J., Impulsive penetration of filamentary plasma elements into the magnetospheres of the Earth and Jupiter, *Planet. Space Sci.*, 25, 887-890, 1977.

Lundin, R., Plasma composition and flow characteristics in the magnetospheric boundary layers connected to the polar cusp, in *The Polar Cusp*, edited by J. A. Holtet and A. Egeland, pp. 9-32, D. Reidel, Norwell, Mass., 1985.

Lundin, R., G. Gustafsson, A. I. Eriksson, and G. Marklund, On the importance of high-altitude low-frequency electric fluctuations for the escape of ionospheric ions, *J. Geophys. Res., 95*, 5905-5919, 1990.

Lundin, R., J. Woch, and M. Yamauchi, The present understanding of the cusp, in Proceedings of the Cluster Workshop, *Eur. Space Agency Spec. Publ., ESA SP-330*, 83-95, 1991.

Maynard, N. C., T. L. Aggson, E. M. Basinska, W. J. Burke, P. Craven, W. K. Peterson, M. Sugiura, and D. R. Weimer, Magnetospheric boundary dynamics: DE 1 and DE 2 observations near the magnetopause and cusp, *J. Geophys. Res., 96*, 3505-3522, 1991.

McDiarmid, I. B., J. R. Burrows, and M. D. Wilson, Large-scale magnetic field perturbations and particle measurements at 1400 km on the dayside, *J. Geophys.*

Res., 84, 1431-1441, 1979.

Newell, P. T., and C.-I. Meng, Cusp width and *Bz*: Observations and a conceptual model, *J. Geophys. Res., 92*, 13673-13678, 1987.

Newell, P. T., and C.-I. Meng, Hemispherical asymmetry in cusp precipitation near solstices, *J. Geophys. Res., 93*, 2643-2648, 1988.

Newell, P. T., and C.-I. Meng, Ionospheric projections of magnetospheric regions under low and high solar wind pressure conditions, *J. Geophys. Res.*, 99, 273-286, 1994.

Nilsson, H., S. Kirkwood, L. Eliasson, O. Norberg, J. Clemmons, and M. Boehm, The ionospheric signatures of the cusp: A case study using Freja and the Sondrestrom radar, *Geophys., Res. Lett., 21*, 1923-1926, 1994.

Norberg, O., M. Yamauchi, L. Eliasson, and R. Lundin, Freja observations of multiple injection events in the cusp, *Geophys. Res. Lett., 21*, 1919-1922, 1994.

Ohtani, S., T. A. Potemra, P. T. Newell, L. J. Zanetti, T. Iijima, M. Watanabe, M. Yamauchi, R. D. Elphinstone, O. de la Beaujardiere, and L. G. Blomberg, Simultaneous prenoon and postnoon observations of three field-aligned current systems from Viking and DMSP-F7, *J. Geophys. Res., 100*, 119-136, 1995.

Potemra, T. A., L. J. Zanetti, R. E. Erlandson, P. F. Bythrow, G. Gustafsson, M. H. Acuña, and R. Lundin, Observations of large-scale Birkeland currents with Viking, *Geophys. Res. Lett., 14*, 419-422, 1987.

Potemra, T. A., R. E. Erlandson, L. J. Zanetti, R. L. Arnordy, J. Woch, and E. Friis-Christensen, The dynamic cusp, *J. Geophys. Res., 97*, 2835-2844, 1992.

Reiff, P. H., T. W. Hill, and J. L. Burch, Solar wind plasma injection at the dayside magnetospheric cusp, *J. Geophys. Res., 82*, 479-491, 1977.

Sandholt, P. E., C. S. Deehr, A. Egeland, B. Lybekk, R. Viereck, and G. J. Romick, Signatures in the dayside aurora of plasma transfer from the magnetosheath, *J. Geophys. Res., 91*, 10,063-10,079, 1986.

Smith, M. F., and M. Lockwood, The pulsating cusp, *Geophys. Res. Lett., 17*, 1069-1072, 1990.

Stasiewicz, K., A global model of gyroviscous field lines merging at the magnetopause, *J. Geophys. Res., 96*, 77-86, 1991.

Walters, G. K., On the existence of a second standing shock wave attached to the magnetosphere, *J. Geophys. Res., 71*, 1341-1344, 1966.

Woch, J., and R. Lundin, Magnetosheath plasma precipitation in the polar cusp and its control by the interplanetary magnetic field, *J. Geophys. Res., 97*, 1421-1430, 1992a.

Woch, J., and R. Lundin, Signature of transient boundary layer processes observed with Viking, *J. Geophys. Res., 97*, 1431-1447, 1992b.

Woch, J., M. Yamauchi, R. Lundin, T. A. Potemra, and L. J. Zanetti, The low-latitude boundary layer at mid-altitudes: Relation to large-scale Birkeland currents, *Geophys. Res. Lett., 20*, 2251-2254, 1993.

Yamauchi, M., Gradual penetration of IMF B_y-component into the cusp and associated field-aligned current, *Mem. Natl. Inst. Polar Res. Spec. Issue Jpn., 36*, 222-231, 1985.

Yamauchi, M., Numerical simulation of large-scale field-aligned current generation from finite-amplitude magnetosonic waves, *Geophys. Res. Lett., 21*, 851-854, 1994.

Yamauchi, M., and R. Lundin, A narrow region of electron beams at the poleward edge of the cusp, *J. Geophys. Res.*, 98, 7585-7591, 1993.

Yamauchi, M., and R. Lundin, Classification of large-scale and meso-scale ion dispersion patterns observed by Viking over the cusp-mantle region, in *Physical signatures of magnetospheric boundary layer process*, edited by J. A. Holtet, and A. Egeland, pp. 99-109, Kluwer Academic Publishers, Dordrecht, Netherlands, 1994.

Yamauchi, M., R. Lundin, and J. Woch, The interplanetary magnetic field B_y effects on large-scale field-aligned currents near local noon: Contributions from cusp part and noncusp part, *J. Geophys. Res.*, 98, 5761-5767, 1993a.

Yamauchi, M., R. Lundin, and A. T. Y. Lui, Vorticity equation for MHD fast waves in geospace environment, *J. Geophys. Res.*, 98, 13523-13528, 1993b.

———

R. Lundin and M. Yamauchi, Swedish Institute of Space Physics, Box 812, S-98128 Kiruna, Sweden. (internat: yamau@irf.se)

T. A. Potemra, Applied Physics laboratory, Johns Hopkins University, Johns Hopkins Road, Laurel, MD 20723-6099.

YAMAUCHI ET AL.: HYBRID CUSP
YAMAUCHI ET AL.: HYBRID CUSP
YAMAUCHI ET AL.: HYBRID CUSP
YAMAUCHI ET AL.: HYBRID CUSP
YAMAUCHI ET AL.: HYBRID CUSP
YAMAUCHI ET AL.: HYBRID CUSP
YAMAUCHI ET AL.: HYBRID CUSP
YAMAUCHI ET AL.: HYBRID CUSP
YAMAUCHI ET AL.: HYBRID CUSP
YAMAUCHI ET AL.: HYBRID CUSP
YAMAUCHI ET AL.: HYBRID CUSP
YAMAUCHI ET AL.: HYBRID CUSP

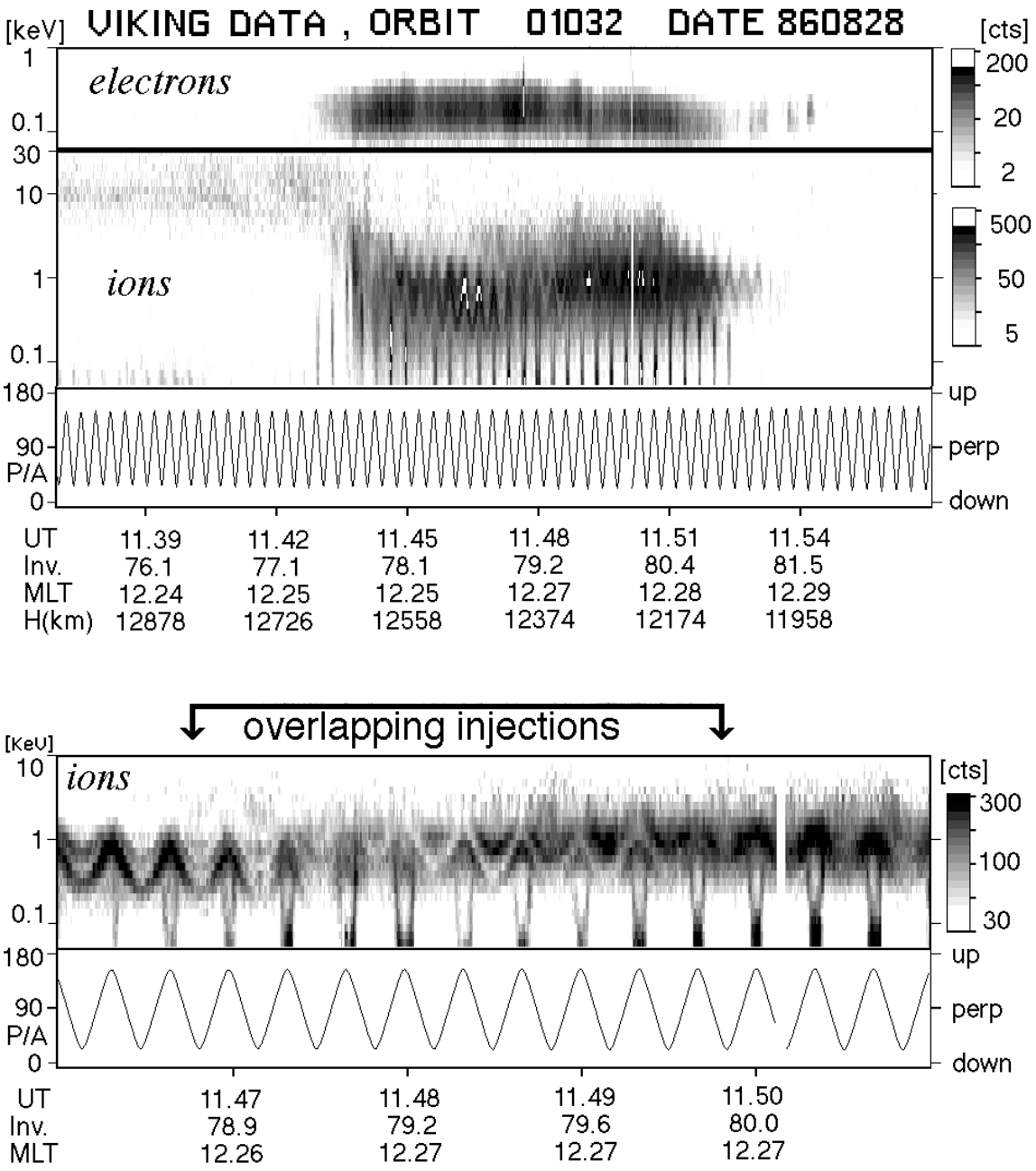

Plate 1. Viking energy-time spectrograms for electrons (70 - 500 eV) and ions (50 eV - 30 keV) of orbit number 1032 during a poleward cusp traversal on August 28, 1986. The cusp is observed at 1143-1154 UT, first strongly affected by southward IMF (1143-1150 UT), then strongly affected by steady northward IMF (1147-1153 UT). The ion data is enlarged in the lower panel. The magnetic field data (northward and westward) are also shown with thin solid lines. Vertical dashed line denotes the stating time of the second particle signature. Positive (negative) slopes correspond to downward (upward) currents. The thick solid line outlines the large-scale profile

which agrees with *Iijima and Potemra* [1976], whereas the dotted line extracts a possible IMF B_y effect which is expected to be carried by the poleward plasma population. Note that the base line (offset line) of the magnetic field at this altitude is rather difficult to determine, and we used a model magnetic field for such a base line. However, the offset line most likely declines as is seen from the difference between the left and right ends of the plate (magnetic field values are different). Once such a corrected offset line is used (see Plate 1 of *Ohtani et al*. [1995]), the existence of a cusp region 0 FAC (1145-1154 UT) becomes more apparent.

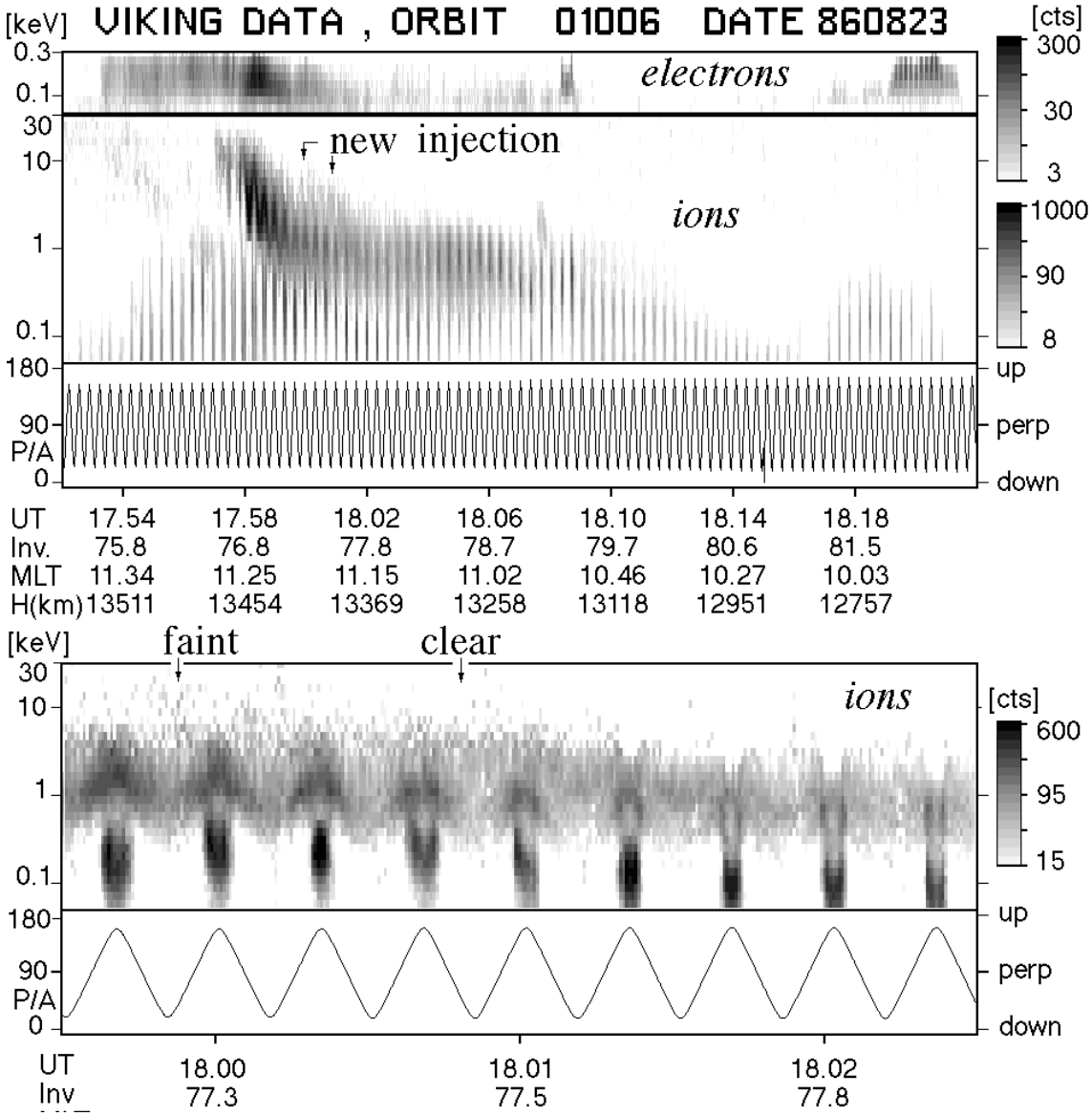

Plate 2. Data for orbit 1006 on August 23, 1986, shown in the same format as Plate 1. The particle signatures are strongly affected first by a southward IMF (before 1800 UT), then by a northward IMF (after 1802 UT). The transition (1800 UT) is marked by a weak discontinuity of particle injection which is accompanied by a strong field-aligned current.

Figure 1. IMP 8 observation of solar wind parameters and IMF (linear scales) from 1000 UT to 1200 UT on August 28, 1986. The IMP 8 satellite is located around X = +26 R_E (front side), Y = −30 R_E (dawnside) and Z = +0.3 R_E in GSM coordinates. The direction of the IMF sharply changed from steady southward (B_z = −5 nT) to steady northward (B_z = +5 nT) at 1125 UT and back to steady southward (B_z = −4 nT) at 1142 UT, whereas the total magnetic field (7 to 8 nT), the solar wind density (6 to 7 × 10^6 m^{-3}), and the bulk velocity (560 to 580 km/s) remained fairly constant. The *AE* index during this period is very quiet (about 100 nT from 0600 UT to 1200 UT).

Figure 2. A possible interpretation of the Viking cusp observation shown in Plate 1. The satellite detected a dynamic response of the cusp when the IMF jumped from steady southward to steady northward. The leading edge and terminating edge are indicated by heavy and light dashed lines, respectively. The light dashed lines indicate the end of the old plasma population associated with southward IMF. Note that the hatched area indicates a plasma population affected by northward IMF, not mixed IMFs. When Viking reached the equator boundary of the cusp at 1143 UT (left), the cusp is affected by southward IMF. Meanwhile, a new injection of northward IMF type started to precipitate, and it finally reached the Viking altitude at 1147 UT. Yet the old plasma population remains until it is swept away at 1150 UT. Then the cusp was characterised by a northward IMF. Note that the cusp location moved poleward by a few degrees because of northward IMF. The "overlapping injections" are seen between the heavy and light dashed lines.

Figure 3. (a) Another possible interpretation of Plate 1. The Viking satellite observed basically the spatial structure, i.e., the satellite moves faster than the dynamical change of the cusp morphology. For the present IMF cases, the equatorward plasma population can be (b) the first southward IMF period (same as Figure 2) or (c) the second southward IMF period. The "overlapping injections" are seen at the area between the heavy and light lines.

Figure 4. A possible scenario of cusp dynamics for the data shown in Plate 1 in terms of the wave-assisted cusp model [*Yamauchi and Lundin*, 1994]. When the sector boundary reaches the cusp boundary (left) which is assumed to standing at high-latitude, the sector boundary can pass through the cusp boundary (middle). Then the cusp boundary begins to move poleward (middle to right). We may than obtain the cusp plasma injection and sweep off old plasma population (cf. Figure 2).